Medical & Biological Engineering & Computing (2019) 57:741–755
https://doi.org/10.1007/s11517-018-1914-0

ORIGINAL ARTICLE

A unified non-linear approach based on recurrence quantification analysis and approximate entropy: application to the classification of heart rate variability of age-stratified subjects

Vikramjit Singh [1] · Amit Gupta [1] · J. S. Sohal [2] · Amritpal Singh [3]

Received: 3 August 2017 / Accepted: 9 October 2018 / Published online: 3 November 2018

Abstract
This paper presents a unified approach based on the recurrence quantification analysis (RQA) and approximate entropy (ApEn) for the classification of heart rate variability (HRV). In this paper, the optimum tolerance threshold (r_{opt}) corresponding to $ApEn_{max}$ has been used for RQA calculation. The experimental data length (N) of RR interval series (RR_i) is optimized by taking r_{opt} as key parameter. r_{opt} is found to be lying within the recommended range of 0.1 to 0.25 times the standard deviation of the RR_i, when $N \geq 300$. Consequently, RQA is applied to the age stratified RR_i and indices such as percentage recurrence (%REC), percentage laminarity (%LAM), and percentage determinism (%DET) are calculated along with $ApEn_{max}$, r_{opt}^{min}, r_{opt}^{max}, and an index namely the radius differential (R_D). Certain standard HRV statistical indices such as mean RR, standard deviation of RR (or NN) interval (SDNN), and the square root of the mean squared differences of successive RR intervals (RMSSD) (Eur Hear J 17:354–381, 1996) are also found for comparison. It is observed that (i) R_D can discriminate between the elderly and young subjects with a value of 0.1151 ± 0.0236 (mean ± SD) and 0.0533 ± 0.0133 (mean ± SD) respectively for the elderly and young subjects and is found to be statistically significant with $p < 0.05$. (ii) Similar significant discrimination was obtained using r_{opt}^{min} with a value of 0.1827 ± 0.0382 (mean ± SD) and 0.2248 ± 0.0320 (mean ± SD) (iii) other significant indices were found to be %REC, %DET, %LAM, SDNN, and RMSSD; however, $ApEn_{max}$ was found to be insignificant with $p > 0.05$. The above features of RR_i time series were tested for classification using support vector machine (SVM) and multilayer perceptron neural network (MLPNN). Higher classification accuracy was achieved using SVM with a maximum value of 99.71%.

Keywords Heart rate variability · Autonomic nervous system (ANS) · Non-linear methods · Information theory · Approximate entropy · Recurrence quantification analysis · Support vector machine

1 Introduction

Heart rate variability (HRV) is the variation in the time interval between successive R-peaks of an electrocardiogram (ECG) signal. The study of HRV is useful in the diagnosis and prognosis of various physiological and pathophysiological conditions [1–4]. HRV is a result of the dynamic interactions between several feedback loops regulating the cardiovascular system occurring at variable rates. This leads to dynamic complexity in the HRV that is altered under different physiological and pathophysiological conditions [5]. It has been established that HRV is altered by several factors like respiratory sinus arrhythmia (RSA); Valsalva maneuver; decreases in venous return, the baroreflex, and the vasovagal reaction; exercise; thermo-regulation; embolisms; intra-venous (IV) injections; circadian rhythms; inter-patient factors like genetics and family history, sex, age, medical condition, and level of fitness; emotion; stress; sleep; body posture; smoking; caffeine; humoral factors, etc. [1–5]. Genesis of HRV is a highly interdependent and complex phenomenon that involves the interactions among parasympathetic and sympathetic branches of

✉ Vikramjit Singh
vikramjit10070@davuniversity.org; vikramkang@gmail.com

[1] Department of Electronics and Communication Engineering, I K G Punjab Technical University, Jalandhar, Punjab, India

[2] Ludhiana College of Engineering and Technology, Ludhiana, Punjab, India

[3] Department of Electrical Engineering, I K G Punjab Technical University, Jalandhar, Punjab, India

ANS along with inputs from the hemodynamic, electrophysiological, and humoral systems [6]. It has been established that measurement and evaluation of cardiovascular complexity from HRV provides useful prognostic indicators [2, 5, 7]. The complexity of beat-to-beat HRV varies with the different physiological situations including disease [8], pharmaceutical interventions [9, 10], and postural changes [11, 12]. Several linear and non-linear methods have been employed in the past to assess the dynamic properties of this physiological time series [13–15]. Linear methods which were based on either time domain [1], frequency domain [16], or time-frequency domain [13, 14, 17] were initially used for the analysis of HRV. Though these methods were able to comprehend the steady-state relation between parasympathetic nervous system and sympathetic nervous system of the ANS that cause HRV pattern, but they were not able to quantify the dynamic behavior of HRV that involved non-linear components of signal generation. Later, non-linear methods like Poincaré plot [18], and certain entropy measures like approximate entropy (ApEn), sample entropy (SampEn) [19], and transfer entropy (TE) [11] were used to characterize complexity of the physiological time series. Lake [20] discovered Gaussianity of HR which is a measure of physiological complexity using Shannon or differential and conditional Renyi entropy rate. Other non-linear methods like phase synchronization, fractal dimension [21], de-trended fluctuation analysis (DFA) [22], and recurrence quantification analysis (RQA) [23] were also used to give deeper insight into the dynamic interactions of HRV.

Beckers [24] concluded that non-linear heart rate fluctuations decline with age due to decreased autonomic modulation with increase in age. This provided evidence for the involvement of the autonomic nervous system in the generation of the complex fluctuation of HRV. Iyenger et al. [25] proved that young subjects have a stronger stability between many different physiological inputs that operate over different time scales so as to regulate cardiac cycle times. In contrast, elderly subjects exhibit crossover behavior due to degradation of some of these inputs and dominance of others. Y. Shiogai et al. [7] confirmed that the SDNN decreases significantly with age irrespective of the gender. Also, the total energy of HRV decreases with age as the influence due to respiratory activity and myogenic activity decreases with age while the neurogenic control of HR becomes more prominent with increasing age. Kampouraki et al. [26] extracted various statistical and wavelet features and utilized SVM for the successful classification of HRV on age-stratified data.

From these studies, it can be inferred that it is very important to take age into consideration for the HRV indices to produce an accurate interpretation in a clinical condition.

The reported studies utilized the established techniques for the quantification of the HRV. This work emphasizes on giving new insights to the quantification of HRV indices of healthy elderly and young subjects by tuning the conventional techniques for optimum results. Time domain indices, descriptive statistics, complexity indices based on ApEn, and non-linear indices based on RQA are analyzed and combined to develop new indices to quantify HRV. Further, a classification method based on support vector machine (SVM) and multi-layer perceptron neural network (MLPNN) is presented to classify the elderly and young subjects.

2 Materials and methods

2.1 Experimental data

Twenty young subjects aged 28 ± 8 (mean ± SD) along with 20 elderly subjects aged 65 ± 5 (mean ± SD) participated in the study. They were abstained from any kind of prescribed medicine, alcohol, tobacco, and caffeine for 12 h prior to the recording. Recordings were done in a quiet and dark room. All subjects were rested initially for 10 min before the start of recording. All subjects were healthy and declared to assume no medication. Continuous ECG signal was recorded for the subjects using MP150 Biopac® System for a duration of 30 min at a sampling frequency of 250 Hz.

2.2 The Fantasia dataset

The Fantasia database from the PhysioBank [25] is an age-stratified data repository to study the effect of age on HRV. It consists of 40 subjects (20 young and 20 elderly) for which 120-min ECG recordings were performed. For 20 young subjects, the age lies between 21 to 34 years and for 20 elderly subjects, the age lies between 68 to 85 years old. Each group consists of healthy subjects that comprise the same numbers of men and women. While recording the ECG, all subjects were kept in a resting supine position in sinus rhythm and subjects watched the movie Fantasia (Disney 1940) to help retain wakefulness. The continuous ECG was sampled at sampling frequency of 250 Hz.

2.3 Extraction of beat-to-beat HRV series

R-peak detection from the ECG was done by an algorithm based on Shannon entropy and Hilbert transform [27]. Ectopic beats, if present, were removed using zero-degree interpolation. From the identified R-peaks of ECG, a time series of RR intervals (RR_i), known as tachogram, is formulated. RR_i thus obtained is the function of the number of heartbeats rather than their time of occurrence.

2.4 Calculation of descriptive statistical features of HRV

In this paper, three descriptive statistical features are evaluated for the HRV. Mean RR is defined as averaged value of the RR_i. SDNN is the standard deviation of the RR_i and RMSSD is defined as root mean square of successive differences of RR_i.

2.5 Calculation of approximate entropy

Approximate entropy (ApEn) is an entropy-based technique, governed by the parameters such as tolerance threshold (r), lag (τ), embedding dimension (m), and data length (N). All these inputs need to be fixed before the calculation of ApEn. This technique is used to quantify the similarity in any time series [19].

Given a time series, $\{d\,(i) : 1 \le i \le N\}$, template vectors $X_1^m, X_2^m, X_3^m \cdots, X_{N-m+1}^m$ are formed where:

$$X_i^m = \{d(i), d(i+\tau), \ldots, d(i+(m-1)\times\tau)\} \tag{1}$$

for $i = 1, 2, \ldots, N-m+1$. The conditional measure (R), so that the distance between two such vectors, within threshold (r), is given by:

$$R_{\mathrm{ij}} = \theta\left(r - \left\|X_i^m - X_j^m\right\|\right) \tag{2}$$

where $\|.\|$ is the maximum norm distance between the two vectors X_i^m and X_j^m and θ (.) is the Heaviside function. The conditional probability, $C_i^m(r)$, defined as the number of such vectors, X_j^m within r of X_i^m, hence is given by

$$C_i^m(r) = \frac{R_{ij}}{N-m+1} \tag{3}$$

where j ranges from *1* to $N-m+1$.

ApEn is computed using the conditional probabilities for m and $m+1$ embedding dimension, given by

$$\mathrm{ApEn}(m,r) = \frac{\sum_{i=1}^{N-m+1} ln\left(\frac{C_i^m(r)}{N-m+1}\right)}{N-m+1} - \frac{\sum_{i=1}^{N-m} ln\left(\frac{C_i^{m+1}(r)}{N-m}\right)}{N-m} \tag{4}$$

ApEn is a biased technique which while calculating conditional probabilities includes self-matching templates. In order to reduce this bias, self-matches are excluded and resulting undefined conditional probability $C_i^m(r)$ is substituted to 0.5 as a correction strategy [28]. This strategy ensures that even for small data sets the bias can be reduced.

2.6 Recurrence quantification analysis

Recurrence quantification analysis (RQA) is a technique of analysis of non-linear data which quantifies the count and period of recurrences of a dynamic system given by its state-space trajectory. Quantification analysis of recurrence plots was first performed by Zbilut and Webber Jr. [29] and was complemented with new complexity measures by Marwan et al. [30].

The calculation of R_{ij}, when both i and j ranges from 1 *to* $N-m+1$, results in a two-dimensional binary $M \times M$ matrix, where, $M = N-m+1$. This two-dimensional matrix is called as recurrence plot (RP). Hence, RP is the recurrence of a state occurring at time i that recur at time j, represented with dots within a two-dimensional squared matrix R_{ij}, as shown in Fig. 1 where both axes are time axes with i and j representing time instants [29].

RQA of recurrence plots is done by measuring the various indices. The typical indices are recurrence rate (%REC), determinism (%DET), and laminarity (%LAM). Recurrence rate (%REC) is the density measure of the points of recurrence in the RP. It is calculated simply by counting the black dots in the RP.

$$\%\mathrm{REC} = \frac{1}{M \times M} \sum_{i,j=1}^{M} R_{\mathrm{ij}} \times 100 \tag{5}$$

Determinism (%DET) is developed to measure the deterministic nature of the signal. In an RP, the diagonal points represent the repeating dynamics of the signal. %DET is defined as the fraction of recurrence points that make diagonal line segments.

$$\%\mathrm{DET} = \frac{\sum_{L=\mathrm{Lmin}}^{M} lPl(l)}{\sum_{i,j=1}^{M} R_{ij}} \times 100 \tag{6}$$

Where Pl(l) gives the number of the diagonal lines of length l, while Lmin is the minimum length of the diagonal lines that have been considered.

%LAM is defined as the proportion of recurrence points that constitute vertical lines in the RP. Laminarity represents random dynamics in the signal.

$$\%\mathrm{LAM} = \frac{\sum_{v=\mathrm{Vmin}}^{M} \mathrm{vPv}(v)}{\sum_{i,j=1}^{M} R_{\mathrm{ij}}} \times 100 \tag{7}$$

where Pv(v) is the count of the vertical lines of length v and Vmin is the minimum length of the vertical lines that have been considered.

2.7 Multilayer perceptron neural network

For short term datasets, multilayer perceptron neural network (MLPNN) classifier is employed which is a commonly used

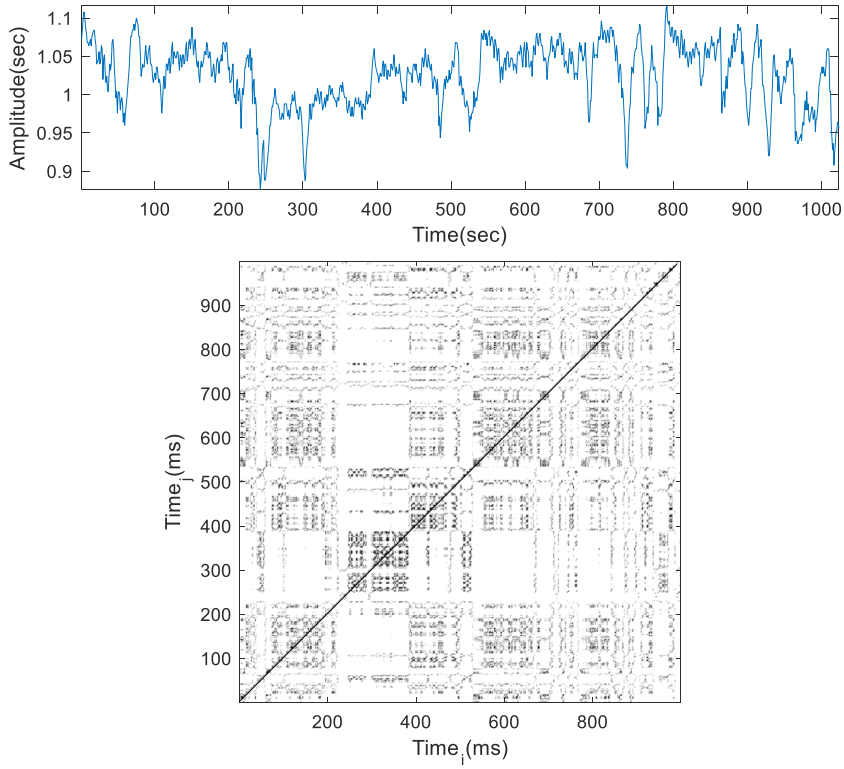

Fig. 1 RR_i series of a typical subject and its corresponding recurrence plot ($m = 2$, $\tau = 1$, $r = 0.2 \times$ SD of time series). Self-matches form diagonal line as shown

feed-forward neural network-based classifier that is simple to implement and is fast in operation [31]. The MLPNN consists of three layers in series: input layer, hidden or concealed layer, and the output layer. The objective of the hidden layer is to receive information from input layer, process it, and to forward it to the output layer. For MPLNN, the amount of neuron in the hidden layer is very critical as insufficient or excessive neurons can cause problems of over fitting [31]. Number of neurons in the hidden layer analytically rather is based on trial and error method [31–34]. For this study, we used a MLPNN model with single hidden layer of five hidden neurons as employed in some of the previous studies [31, 35].

The neurons which are in the middle layer multiply the input X_i with their connection weights W_{ij} and sum them up as per the following equation (Fig. 2).

$$Y_j = \varnothing\left(\sum X_i W_{ij}\right) \tag{8}$$

Here, $\varnothing$ is an activation function which can be threshold function, sigmoidal function, or hyperbolic tangent function [31]. In this study, a hyperbolic tangent function has been employed as the activation function [31]. In MLPNN, each weight W_{ij} is adjusted iteratively so as to reduce the error (E) between the actual response Y_j and desired response Y_{dj}. E is defined as

$$E = \frac{1}{2}\left(Y_{dj} - Y_j\right)^2 \tag{9}$$

For adjusting the weights and minimizing the error, many training algorithms have been employed and out of these, a commonly used one is backpropagation (BP) training algorithm. In this paper, backpropagation supported by the Levenberg–Marquardt (LM) algorithm [31–34] has been employed to address the problem of slow convergence of conventional BP algorithm.

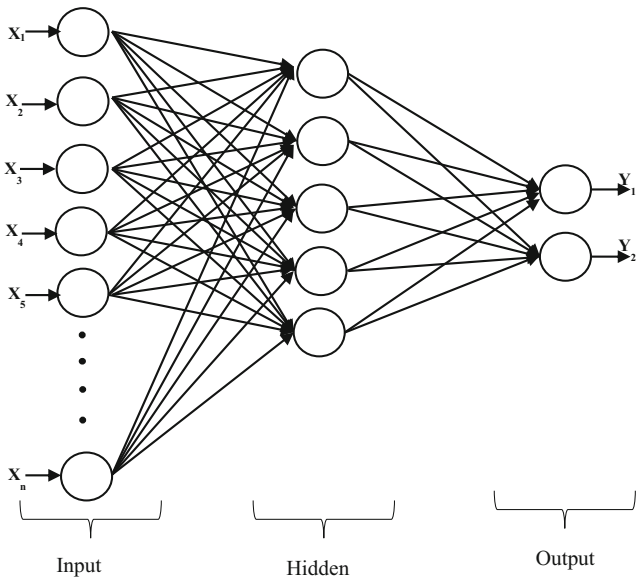

Fig. 2 The structure of the MPLNN model

2.8 Support vector machine

Support vector machine (SVM) is an algorithm of machine learning, that is used for classification and regression purposes [36]. It is a form of supervised learning that is based on statistical learning theory. SVM is based on the idea of finding a hyper plane that discriminates the data into distinct classes where data is projected into a higher dimensional feature space. SVM distinguishes the data by maximizing the margin and minimizing the class error ratio [37]. SVM comprises of many reliable properties for learning and provides good experimental results, so it finds many applications in various fields [26, 36, 38, 39].

Figure 3 presents the basic idea about SVM. The data points are classified as positive or negative by finding a hyper plane that separates the data points my maximum margin.

For further explanation, suppose x is a vector which denotes a pattern to be classified and d denotes its class ($d \in \{\pm 1\}$). Also let ($\{x_i, d_i\}$, $i = 1, 2, \ldots\ldots. k$) denotes a set of k training examples. In SVM, the challenge lies with the creation of a decision variable, $f(x)$, that it correctly categorizes data into two classes. For linear SVM classifiers, the decision variable is given as [26]

$$f(x) = W^T x + b \tag{10}$$

such that $d_i f(x_i) > 0$ for $d_i = +1$ and $d_i f(x_i) < 0$ for $d_i = -1$, where W is the vector of weights and while b defines the bias that forms the hyper plane, $f(x) = 0$. In SVM, the optimal hyper plane with maximum class separation can be found by lessening the following cost function [26]

$$j(w) = \frac{1}{2} W^T W = \frac{1}{2} \|W\|^2 \tag{11}$$

subject to the constraints of separation

$$d_i\left(W^T x_i + b\right) \geq 1 \; for \;\; i = 1, 2, \ldots\ldots\ldots\ldots k \tag{12}$$

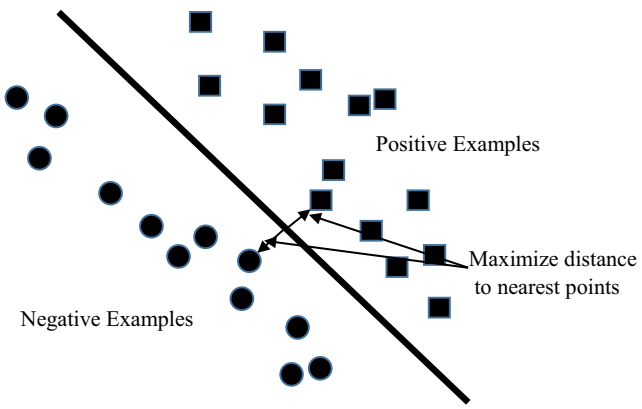

Fig. 3 SVM classification

Solution to (11) is given by

$$W = \sum_{i=1}^{k} (\alpha_i d_i x_i) \tag{13}$$

Hence, the final decision variable can be obtained by

$$f(x) = \text{sign}\left(\sum_{i=1}^{k} (\alpha_i d_i x x_i + b) \right) \tag{14}$$

where x_i is the training vector, x is the classification vector, and α_i are the langrage multipliers for enhancing separation.

For the classes which are not linearly separable, kernel function $k(x, x_i)$ is used, which facilitates the classification using linear hyper plane. The final decision function given in (14) is adapted to

$$f(x) = \text{sign}\left(\sum_{i=1}^{k} (\alpha_i d_i \text{k}(x, x_i) + b) \right) \tag{15}$$

The kernel function of the SVM can be linear, polynomial, Gaussian, radial function etc. In this paper, for the choice of the SVM kernel, SVMs with various kernels like linear SVM, cubic SVM, quadratic SVM, fine Gaussian SVM, medium Gaussian SVM, and course Gaussian SVM were tested for the classification at it was found that SVM with quadratic kernel provides the highest accuracy [23].

2.9 Statistical analysis

A comparison among the different indices for the elderly and young subjects is performed using normal distribution and variance homogeneity test. If the results are positive, then independent samples t test is implemented, otherwise Wilcoxon rank test is done for a significance level of 0.05.

2.10 Selection of optimum threshold (r_{opt})

For the calculation of various indices of RQA and ApEn, selection of threshold "r" is very significant. For RQA, researchers have used empirically defined "r" as 0.20–0.25 times the standard deviation of the signal [23, 40]. For calculating ApEn, in case of slow dynamic signals, researchers have prescribed "r" within 0.01.–0.2 times the standard deviation of the signal [41]. Further, Chon et al. [42] illustrated that instead of strictly following the range recommendation, selected "r" should correspond to ApEn_{max}. This choice eliminates the problem of underestimating the ApEn due to lower tolerance as well as intrusion of self-matches in ApEn calculations due to higher tolerance threshold. The selected "r" corresponding to ApEn_{max} is the tipping point where self-matches begin to dominate other matches. Hence, it is the most appropriate measure to quantify the complexity of any time series.

The corresponding "r" is considered as optimum tolerance threshold value, i.e., r_{opt} [41].

In this paper, r_{opt} that corresponds to $ApEn_{max}$ is used for the calculation of RQA indices such as %REC, %DET, and % LAM. The corresponding calculations of ApEn and RQA have been made by selecting low embedding dimension, $m = 2$ and $\tau = 1$ [43]. Figure 4 shows the variation of ApEn with variation in "r" with a step size of 0.01. Corresponding to the $ApEn_{max}$, r_{opt}^{min} and r_{opt}^{max} define the range of the values for the choice of r_{opt}.

RR_i is a time series with finite resolution that is acquired from ECG signal, sampled at finite sampling frequency; therefore, sampling and quantification errors in the discrete RR_i may lead to erroneous ApEn and %REC calculations [44]. This is reflected from the outcomes depicted in Figs. 4 and 5, which show the relationship between the number of neighborhood points and the radius of the neighborhood indicated by stepped line for the variation of ApEn and %REC. These steps lead to different values of r_{opt}, i.e., ranging between r_{opt}^{min} and r_{opt}^{max}. However, for infinite resolution, this stepped response will be replaced by smooth line and r_{opt}^{min} and r_{opt}^{max} will coincide to a single value of r_{opt}.

Figure 5 shows the behavior of r_{opt} for a typical elderly, a young subject, and a random noise (RN) series for the data length (N) of 300. Due to higher resolution of RN series, r_{opt} corresponds to single value, while for RR_i series, r_{opt} is spread over a range of values. It is also seen that for an elderly subject, the minimum value of r_{opt}, i.e., r_{opt}^{min}, is lesser than that of its young counterpart. On the other hand, r_{opt}^{max} of the elderly subject is greater than that of young subject, which results in greater difference between r_{opt}^{min} and r_{opt}^{max} for the elderly subject than young one.

2.11 Selection of appropriate RR data length (*N*)

Calculating ApEn requires comparison of the various data templates derived from a larger dataset having length N. Hence, $ApEn_{max}$ and r_{opt} are critically dependent on N. In this work, N is carefully chosen so that r_{opt} corresponding to $ApEn_{max}$ lies within the suggested range between 0.1 and 0.25 times SD of RR_i [45].

To ascertain the optimum data length to be chosen for r_{opt}, 50 realizations of random noise (RN) of N varying from 50 to 700 in steps of 50 are simulated and the same is performed on real RR_i for young and elderly subjects. Figure 6 shows the variation of r_{opt} with respect to N for RN series. It is observed that r_{opt} decreases with increase in N and becomes nearly constant for $N \geq 300$ for RN series.

Figures 7 and 8 show the variation of r_{opt} with respect to N varying for RR_i obtained from young and the elderly subject respectively. It is seen that the minimum value of N, for which r_{opt} (r_{opt}^{min}) is within the recommended range, is found to be 300 for elder as well as young subjects. In this case also, r_{opt}

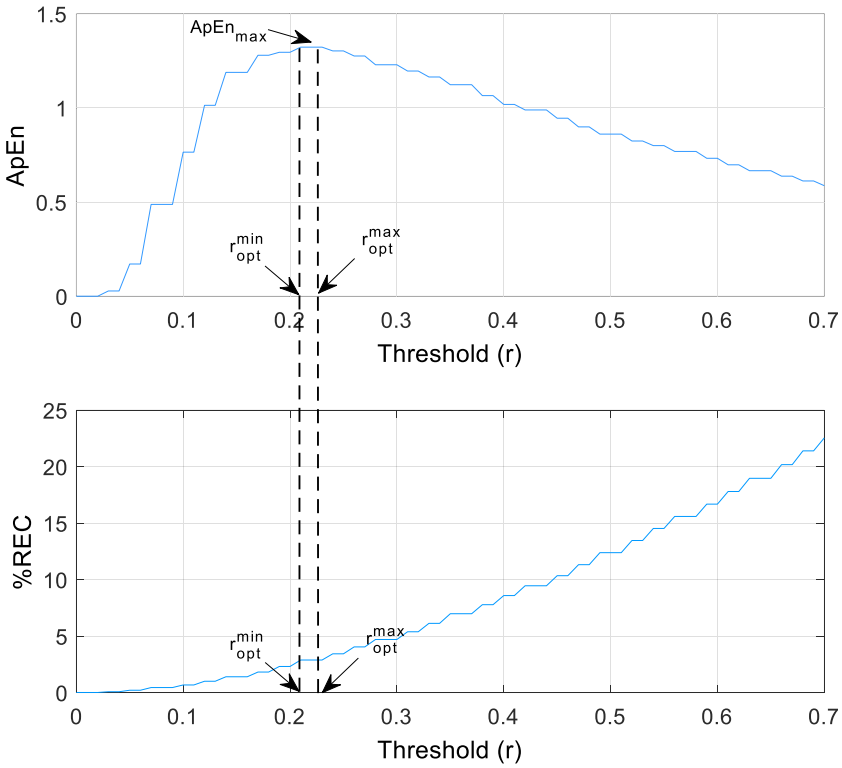

Fig. 4 ApEn and %REC values over the range of "r" varying from 0 to 0.7 in steps of 0.01 for an RR_i, r_{opt}^{min} and r_{opt}^{max} correspond to the maximum value of ApEn depicted as ApEnmax. The corresponding calculation is made by choosing m as 2 and τ as 1

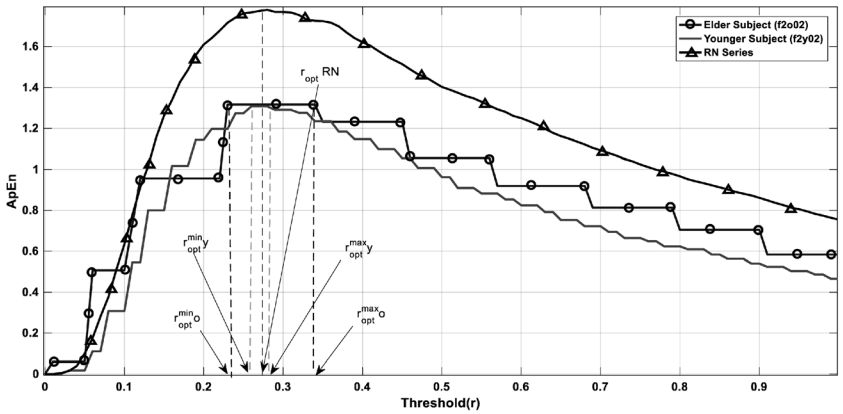

Fig. 5 Selection of r_{opt} for the elderly subject (f2o02) and young subject (f2y02) and random noise (RN), $N = 300$

remains almost constant for $N \geq 300$ and remains within the suggested range for RR_i.

From Figs. 7 and 8, it is also observed that mean value of r_{opt}^{min} remains lower for the elderly subjects irrespective of data length, while on the other hand, mean value of r_{opt}^{max} always remain higher.

2.12 Calculation of radius differential (R_D)

It has been established that due to the finite sampling frequency of ECG, the return map of RR_i as shown in Fig. 9 have points lying at least one sampling period (T_S) apart [44]. This separation increases further, if RR_i time series has lower complexity, due to reduced probability of finding a point at minimum resolution. Based on this, an index, namely radius differential (R_D), is provided for the assessment of complexity. R_D is defined as the range of values of r_{opt} that corresponds to same value of ApEn, i.e., $ApEn_{max.}$

$$R_D = \left(r_{opt}^{max} - r_{opt}^{min}\right) \tag{16}$$

Hence, R_D is the amount of uncertainty involved in calculating r_{opt} within the plateau range $\left(r_{opt}^{max}, r_{opt}^{min.}\right)$

Figure 9 shows the Poincaré plot of RR_i where threshold r_{opt}^{min} and r_{opt}^{max} are represented by two concentric circles. From Fig. 9, it is assumed that the inner and outer circles encompass the same number of points, and hence they correspond to the same value of ApEn. Hence, R_D can be taken as the radial difference between these two concentric circles.

Figure 10 shows the Poincaré plot of an elderly and a young subject from the Fantasia database. The distribution of points is dense for the young subject, which results in lower value of R_D. It is also worth mentioning here that the minimum value of R_D is limited by sampling interval (T_s). Hence, the changes in HRV with age, captured by R_D, are apparent from Figs. 5, 9, and 10

3 Results

3.1 Descriptive statistics (mean ± SD)

The results presented in Table 1 are calculated by randomly extracting 1040 data segments of RR_i with a preset length of 300, from the recorded and standard Fantasia database of the elderly and young subject s. It is observed that for HRV, mean of SDNN is greater in the case of the young subjects than the elderly subjects. The heart rate, represented by reciprocal of

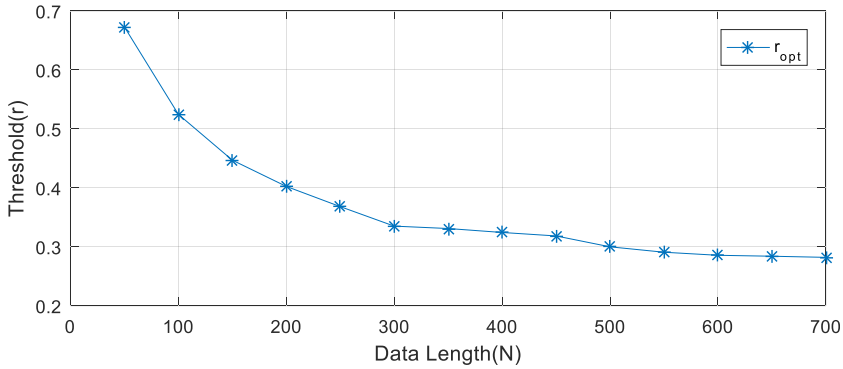

Fig. 6 Variation of mean of "r_{opt}" with data length (N). "r_{opt}" value is mean over 50 random noise (RN) series

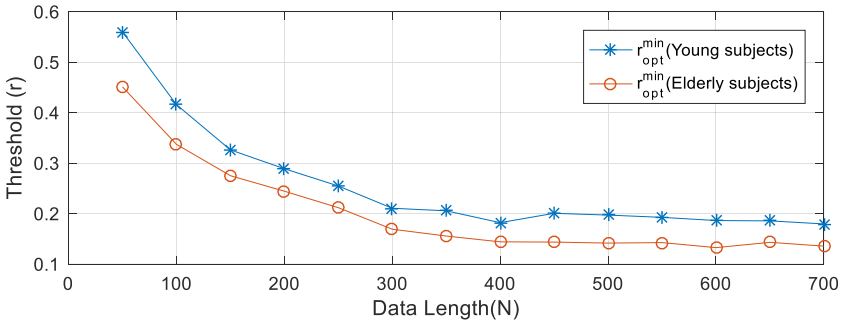

Fig. 7 Variation of mean of lower value of "r_{opt}" (r_{opt}^{min}) with data length N for RR_i

mean RR, is higher in young subjects than those of the elderly subjects. These results were found significant with p value less than 0.05. Figure 11 also endorses the results.

3.2 ApEn results

In this paper, for the calculation of ApEn- and RQA-related indices, $m = 2$, $\tau = 1$, and $N = 300$ are used. The indices calculated from ApEn are tabulated next to the descriptive statistics indices in Table 1. $ApEn_{max}$, r_{opt}^{min}, r_{opt}^{max}, and R_D are computed from the RR_i time series of the elderly and young subjects. Mean and SD of each parameter along with p value are depicted. Mean value of $ApEn_{max}$ is almost similar for the elderly and young subjects with a marginal difference. Averaged r_{opt}^{min} is lower for the elderly subjects than the young ones, while the mean value of r_{opt}^{max} is slightly higher for the elderly subjects. Parameter R_D has a significantly higher mean value for the elderly subjects than the young subjects. All indices are found significant with a lower p value, except $ApEn_{max}$, which has a p value of 0.118.

3.3 RQA results

The indices calculated from RQA are presented next to the ApEn indices in Table 1. Mean and SD of %REC, %DET, and %LAM along with their respective p values are presented. In this paper, for the calculation of %DET and %LAM, minimum line length is set to 3, as this results in the decay in the influence of noise [43]. Mean of %REC is almost the same for the two classes with a slight difference, conversely SD of %REC shows substantial change. Similar trend is observed for %DET and %LAM. These indices are found significant with a lower p value.

3.4 Effect of sampling frequency of ECG on ApEn indices

The values of ApEn indices r_{opt}^{min}, r_{opt}^{max}, and R_D may be influenced by the resolution of RR intervals and hence depend upon sampling frequency of the ECG signal acquired. To investigate this, these indices are computed for the ECG signals sampled at 250 Hz, 500 Hz, and 1000 Hz for the elderly and young subjects respectively. To obtain high-resolution ECG signals, the already acquired ECG signals (sampled at 250 Hz) were interpolated to reflect a sampling frequency of 500 Hz and 1000 Hz using cubic spline interpolation [46]. The results are presented in Table 2.

3.5 Correlation analysis of descriptive statistics, RQA, and ApEn

A correlation analysis between descriptive statistics, RQA, and ApEn indices is carried out for the young and elderly subjects using Pearson's cross correlation coefficient and the results are tabulated in Tables 3, 4, and 5 respectively. Table 3 shows the Pearson cross correlation (CC) between descriptive

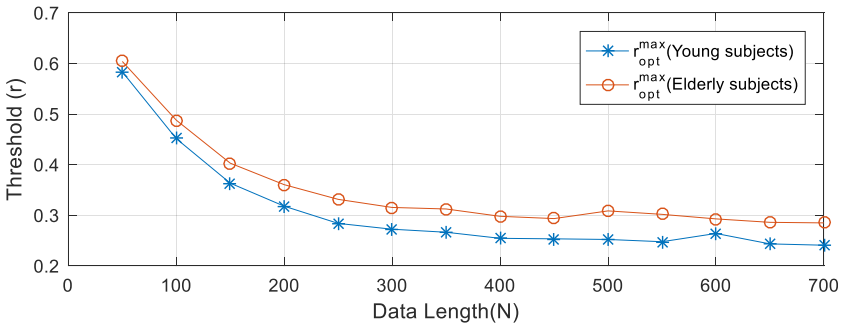

Fig. 8 Variation of mean of upper value of "r_{opt}" (r_{opt}^{max}) with data length N for RR_i

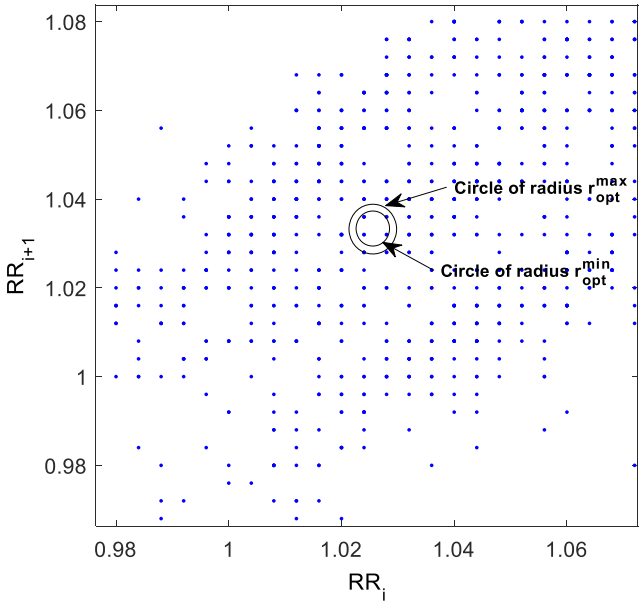

Fig. 9 Poincaré plot of an RR_i, inner and outer circles are drawn with threshold (radii) r_{opt}^{min} and r_{opt}^{max} respectively. Both these circles have encircled the same number of points

statistics and ApEn indices for the elderly and young subjects. Table 4 shows the cross correlation between ApEn and RQA indices. Table 5 shows the cross correlation between RQA indices and descriptive statistics.

3.6 Classification by MLPNN and SVM

In this work, commonly used 10-fold cross-validation has been employed to classify the samples. The significant indices as stated in Table 1, derived from 1040(520 each) data segments for the elderly and young subjects, were used. To examine the effect of the selection of indices on the classification performance, the indices were categorized into three different categories. *Category-I* comprises of descriptive indices such as mean RR, SDNN, and RMSSD. *Category-II* comprises of RQA indices such as %REC, %DET, and %LAM, while *Category-III* consists of ApEn indices such as r_{opt}^{min}, r_{opt}^{max}, and R_D. For comparing the performance of the two classifiers, the following performance measures were employed:

$$\text{Recall} = \frac{\text{True Positive(TP)}}{\text{True Positive(TP)} + \text{False Negative (FN)}} \quad (17)$$

$$\text{Precision} = \frac{\text{True Positive (TP)}}{\text{True Positive (TP)} + \text{False Positive(FP)}} \quad (18)$$

$$\%\text{Accuracy} = \frac{\text{No of Correct decisions}}{\text{Total no of decisions}} \quad (19)$$

Figure 12 presents the variation of various performance measures with the choice of features. It is observed that, considering all the features as input to the classifier, SVM performs better than MLPNN with a maximum *% accuracy* of 99.7, *recall* and *precision* of 0.998 and 0.996 respectively. It is found that while considering *Category-I* along with *Category-III*, viz., leaving out the RQA features, the classification performance is significantly decreased. Similarly, the combination of *Category-II & III* produced a *% accuracy* of 90%, *recall* of 0.896, and *precision* of 0.903 for SVM while *% accuracy* of 85.1%, *recall* of 0.862, and *precision* of 0.864 was observed for MLPNN. Further, a significant drop in *% accuracy*, *recall*, and *precision* was observed both for SVM and MLPNN when ApEn-derived features were omitted, viz., *Category-I* along with *Category-III* was employed. Moreover, for the individual classification performance of the three categories of feature vectors, each category was separately tested and it was found that the *Category-III*, in which ApEn-derived features were present, gave improved results, i.e., *% accuracy* of 84.6 for SVM and 79.6 for MPLNN. The separate test of *Category-I* resulted with *% accuracy* of 81.2% and 78% for SVM and MLPNN respectively. RQA-derived features from *Category-II* were only able to discriminate classes with % accuracy of 68.8% for SVM and 62.1% for MLPNN.

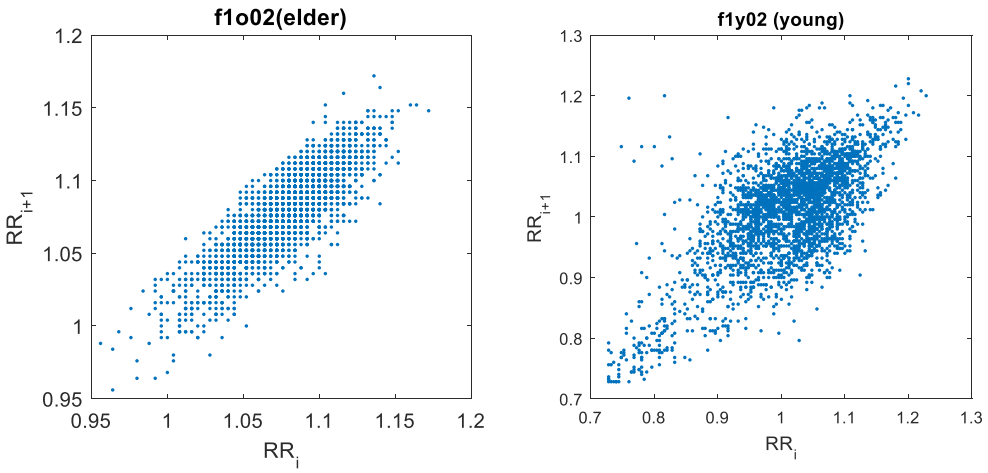

Fig. 10 Poincaré plot of an elderly and a young subject from the Fantasia database

Table 1 Mean and SD of various indices of the young and the elderly subjects calculated for 1040 data segments with $N = 300$, extracted from recorded and fantasia dataset

Measures	Elderly subjects		Young subjects		p value
	Mean	SD	Mean	SD	
Mean RR	1.05	0.15	0.97	0.14	< 0.05
SDNN	0.04	0.02	0.07	0.04	< 0.05
RMSSD	0.02	0.01	0.06	0.04	< 0.05
$r_{\text{opt}}^{\text{min}}$	0.18	0.04	0.22	0.03	< 0.05
$r_{\text{opt}}^{\text{max}}$	0.31	0.05	0.27	0.04	< 0.05
R_{D}	0.12	0.02	0.05	0.01	< 0.05
ApEn_{max}	1.22	0.07	1.23	0.07	0.11
%REC	3.73	1.07	3.40	0.68	< 0.05
%DET	32.41	5.53	30.62	4.33	< 0.05
%LAM	18.51	5.91	12.84	5.39	< 0.05

4 Discussion

In the clinical setting, HRV and its use for predictive purposes is accounted for a number of physiological factors such as age and gender. HRV is known to decrease with normal aging process. This is indicated by the linear and non-linear indexes that reduce with age. This can be related to the concept of decreasing autonomic modulation with advancing age. Moreover, the reduction of the magnitude of heart period fluctuations and the decrease of complexity of the heart period dynamics are interpreted as a sign of the reduction of respiratory sinus arrhythmia and the increased activation of sympathetic control with age [4, 7, 24, 47, 48]. Therefore, it is important to take age into consideration for the HRV indices to produce an accurate interpretation in a clinical condition. The present work aids the previous studies and uses complexity indices that correlate to the descriptive statistics. In the earlier works [4, 12, 24, 47], it has been found that the young and elderly subjects can be differentiated based on HRV statistics; however, present work emphasizes on the development of complexity related indices that can significantly differentiate the two groups even for shorter data sets.

The autonomic nervous system (ANS) possesses a regulatory structure governed by non-linear processes and mechanisms controlled by the brain stem [7]. From Table 1, it is evident that the averaged mean RR of the elderly subjects is higher than that of the young subjects, implying that the heart rate of the young subjects is greater than that of the elderly subjects. Also, the data segments derived from the young subjects have higher averaged SDNN than the elderly subjects confirming greater HRV in the young subjects. Physiologically, this is due to sluggishness in the control mechanisms governing HRV due to aging. This is further confirmed by the higher value of RMSSD in the young subjects. These descriptive statistics alone are not enough to capture the real non-linear characteristics of the ANS processes

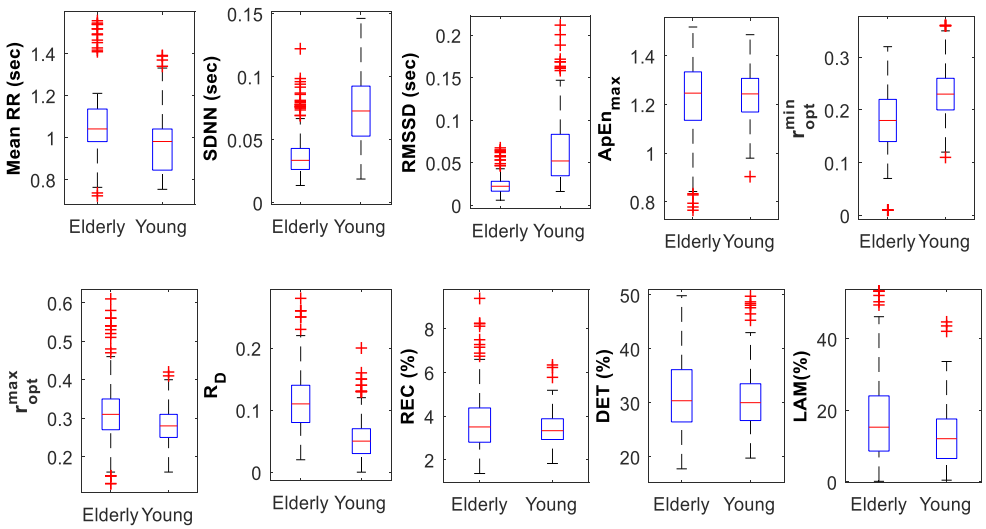

Fig. 11 Indices computed for RR_i time series of the elderly and young subjects from the Fantasia database [43]

Table 2 Effect of sampling frequency of ECG on ApEn indices

Index	Sampling frequency	Elderly subjects		Young subjects		p value
		Mean	SD	Mean	SD	
r_{opt}^{min}	250 Hz	0.1827	0.0382	0.2248	0.0320	< 0.05
	500 Hz	0.1831	0.0490	0.2011	0.0361	< 0.05
	1000 Hz	0.1977	0.0479	0.2094	0.0378	< 0.05
r_{opt}^{max}	250 Hz	0.3080	0.0492	0.2733	0.0362	< 0.05
	500 Hz	0.2653	0.0584	0.2223	0.0382	< 0.05
	1000 Hz	0.2486	0.0527	0.2160	0.0383	0.09
R_D	250 Hz	0.1151	0.0236	0.0533	0.0133	< 0.05
	500 Hz	0.0821	0.0246	0.0211	0.0164	< 0.05
	1000 Hz	0.0509	0.0129	0.0066	0.0082	< 0.05

and controls. To address this issue, the present work utilizes the features obtained from non-linear method of RQA and ApEn to quantify and classify HRV of the young and the elderly subjects. The bias introduced in the ApEn due to the "not defined" conditional probability (CP) is addressed by substituting the CP to 0.5 [28]. A unification approach utilizing the indices obtained from RQA and ApEn is presented to refine the RQA based on optimum threshold values r_{opt}^{min}, r_{opt}^{max} and a newly proposed index R_D.

Considering this, an effort has been made to extract these non-linear features, derived from indices listed in Table 1. In this work, traditional RQA method is fine-tuned by the selection of appropriate threshold based upon the maximum value of ApEn. From Table 1, it can be realized that, there is no substantial difference in the value of $ApEn_{max}$ for the elderly and young subjects, further confirmed by a higher p value. On the contrary, r_{opt}^{min} and r_{opt}^{max} and R_D are found to be significant, having a considerably different values for the elderly subjects and young ones. This is also depicted in the box and whisker plot shown in Fig. 11.

It is observed from Fig. 7 that, irrespective of data length N, r_{opt}^{min} has a lower mean value for the elderly subjects than the young subjects. This is because, for the elderly subjects, self-matches rapidly overpower other matches than the young subjects due to lesser variability in the heart rate of the elderly subjects than the young ones.

From the results shown in Table 2, it can be seen that r_{opt}^{min}, r_{opt}^{max}, and R_D are influenced by the sampling frequency of ECG. However, the indices calculated for a relative study of elderly and young subjects under similar data acquisition techniques still provide significant distinguishing features. The lowest value of R_D, i.e., mean minus the SD, is 0.04 for young subjects at 250-Hz-sampled ECG signal. This value is in fact the resolution of the ECG signal at this sampling rate. However, the value of R_D for elderly subjects is higher than this lower limit of 0.04. Similar results are obtained for ECG sampled at 500 Hz and 1000 Hz. In a more generalized study, it is proposed to sample the ECG signal at a higher rate than 250 Hz to get a good resolution for fast as well as slow changing signals.

From Table 3, it is observed that R_D is significantly correlated (p value < 0.05) to SDNN with a CC value of − 0.8927 and − 0.8597 respectively for elderly and younger subjects. Similarly, it is significantly correlated (p value < 0.05) to RMSSD with a CC value of − 0.6893 and − 0.6632 respectively for the elderly and younger subjects. This drop in SDNN is due to the decrease in HRV with age. R_D being strongly correlated to SDNN and RMSSD shows the similar

Table 3 Pearson cross correlation (CC) between descriptive statistics and ApEn indices for the elderly and young subjects

		r_{opt}^{min}		r_{opt}^{max}		R_D	
		CC	p value	CC	p value	CC	p value
Elderly subjects	Mean RR	0.2386	0.0754	0.2385	0.0875	− 0.1492	< 0.05
	SDNN	0.5994	< 0.05	− 0.6676	< 0.05	− 0.8927	< 0.05
	RMSSD	0.4631	< 0.05	− 0.4290	< 0.05	− 0.6893	< 0.05
Young subjects	Mean RR	0.09961	0.0531	0.0447	0.3090	− 0.0465	0.2893
	SDNN	0.5766	< 0.05	− 0.6057	< 0.05	− 0.8597	< 0.05
	RMSSD	0.5327	< 0.05	− 0.6390	< 0.05	− 0.6632	< 0.05

Table 4 Pearson cross correlation (CC) between ApEn and RQA indices for the elderly and young subjects

		r_{opt}^{min}		r_{opt}^{max}		R_D	
		CC	*p* value	CC	*p* value	CC	*p* value
Elderly subjects	% REC	0.4378	< 0.05	0.5383	< 0.05	0.5310	< 0.05
	% DET	− 0.0930	< 0.05	− 0.0312	0.4776	0.0557	0.2046
	% LAM	− 0.3263	< 0.05	− 0.2572	< 0.05	0.0092	0.8336
Young subjects	% REC	0.4040	< 0.05	0.5427	< 0.05	0.3629	< 0.05
	% DET	− 0.1258	< 0.05	− 0.0420	0.3390	0.0733	0.0948
	% LAM	− 0.3551	<0.05	− 0.2592	< 0.05	0.0644	0.1421

behavior. However, signal amplitude (RR variability amount sized by SDNN) is not coincident with complexity. Linear measures like SDNN does not capture the dynamics involved in the genesis of HRV. Non-linear measures like RQA face the limitation of dimensionality. Complexity-based measures like ApEn are used to characterize these dynamics quantitatively. The utility of R_D is towards the unification of RQA and ApEn and highlighting uncertainty in calculating "r^{opt}," hence provide an alternative index to measure the complexity of HRV. The radius indices r_{opt}^{min} and r_{opt}^{max} show moderate positive and negative correlation with SDNN and RMSSD respectively and that confirms to the results obtained in Fig. 5. From Figs. 5, 9, and 10, it is seen that index R_D, which signifies the uncertainty in calculating r_{opt}, shows a relative difference between the younger and elderly subjects. There is no significant correlation between mean RR and ApEn indices, i.e., r_{opt}^{min} and r_{opt}^{max}. This is because mean RR provides no information about the complexity of the signal. Table 4 shows the cross correlation between ApEn and the RQA indices. A moderate correlation is observed between the %REC, %LAM, r_{opt}^{min}, and r_{opt}^{max} indices. The cross correlation between RQA indices and descriptive statistics is tabulated in Table 5. A significantly lower correlation is observed between these two classes of indices. This is because complexity is a different phenomenon than the amount of variability as measured by the variance and the standard deviation of a signal. Though, SDNN and RMSSD quantify the variations in a signal, these do not quantify the information about recurrence of samples of a given signal as measured by the RQA indices, viz., %REC, %LAM, and %DET.

A classification *% accuracy* of 81.2% is obtained by feeding the descriptive features (*Category-I*) to SVM in comparison to 78% using MLPNN classifier is shown in Fig. 12a. Moreover, from Fig. 12b, c, the *recall* values can be observed as 0.70 and 0.684 and *precision* values of 0.667 and 0.611 respectively for SVM and MLNPP. The classification indices for the quantification of the young vs. the elderly subjects can be enhanced if the non-linear characteristics of ANS control are captured using non-linear and information theory-based techniques such as RQA and ApEn respectively. Similar classification was done using RQA indices (*Category-II*) and a reasonable accuracy was obtained.

A significant improvement in the classification accuracy is observed when r_{opt}^{min}, r_{opt}^{max}, and R_D features (*Category-III*) are used for the classification with *% accuracy* of 84.6% and 79.6% for SVM and MPLNN respectively. The classification accuracy improved further when a combination of two categories of features was used. The best results were obtained when descriptive indices (*Category-I*) were used along with ApEn features (*Category-III*) for the classification with *% accuracy* of 92.8% and 87.2% using SVM and MLPNN respectively.

Lastly, all the features were combined for the classification of data. The classification *% accuracy* of 99.7% was achieved using SVM with *recall* and *precision* values of 0.998 and 0.996 respectively. Using MLPNN resulted in *% accuracy*

Table 5 Pearson cross correlation (CC) between descriptive statistics and RQA indices for the elderly and young subjects

		%REC		%DET		%LAM	
		CC	*p* value	CC	*p* value	CC	*p* value
Elderly subjects	Mean RR	− 0.1159	< 0.05	− 0.1644	< 0.05	− 0.1228	< 0.05
	SDNN	− 0.1469	< 0.05	− 0.0091	0.8344	0.0422	0.3366
	RMSSD	− 0.0781	0.0749	− 0.1586	< 0.05	− 0.2007	< 0.05
Young subjects	Mean RR	− 0.0797	< 0.05	− 0.1764	< 0.05	− 0.1300	< 0.05
	SDNN	− 0.2326	< 0.05	− 0.0104	0.8123	0.0379	0.3878
	RMSSD	− 0.1736	< 0.05	− 0.1607	< 0.05	− 0.2010	< 0.05

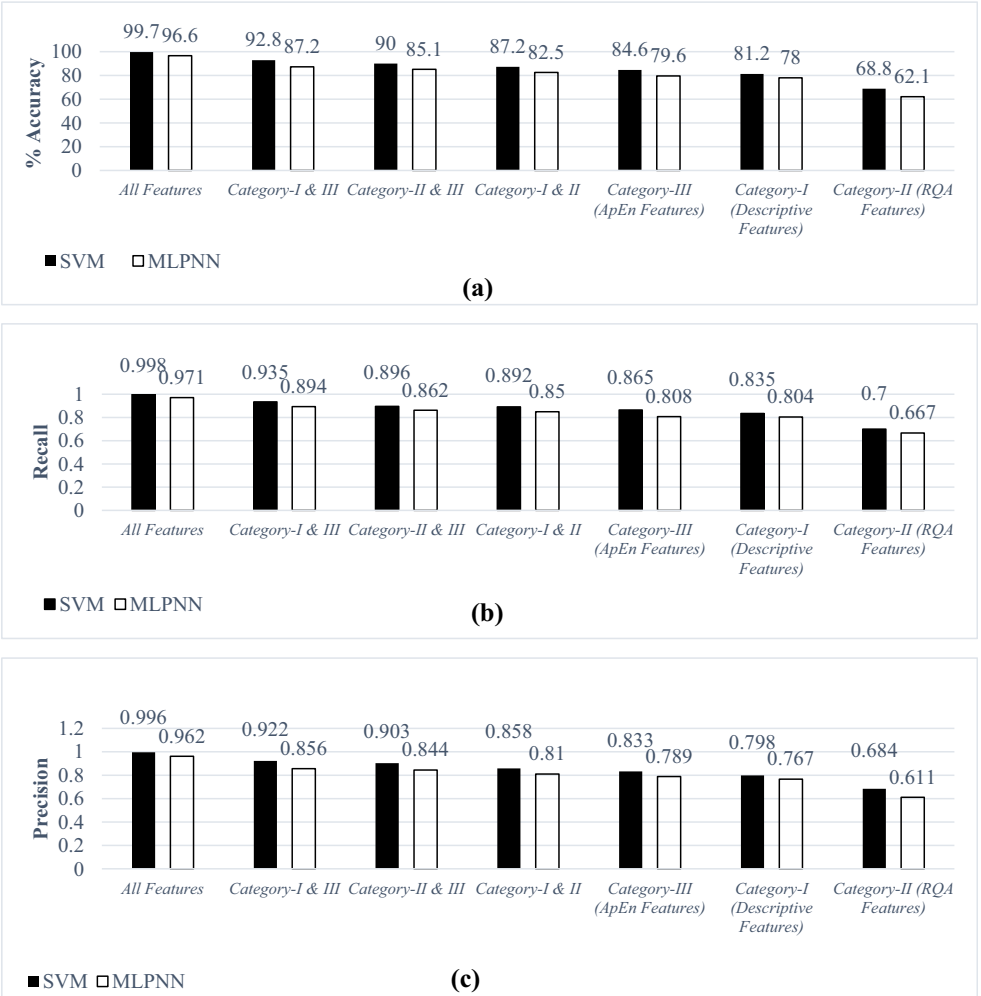

Fig. 12 Classification performance measures as a function of combination of features

of 96.6% with *recall* value of 0.971 and *precision* values of 0.962.

The results of this work are in line with the previous studies reported [7, 24–26, 39, 47, 49]. The decrease in the value of R_D indicates the decreases complexity on HRV series with advancing age as concluded by Y. Shiogai et al. [7], Iyenger et al. [25], Voss et al. [49], and many other researchers. The optimized data length N of 300 for the quantification of HRV by ApEn and RQA confirms the choice of length of RR time series for the HRV analysis as reported in [13, 50, 51]

5 Conclusion

Non-linear physiological control mechanisms associated with ANS are captured by adding the indices obtained from non-linear and information-based methods to the traditional descriptive statistics used for quantification of HRV. Enhanced classification accuracy is observed using the combination of these indices to segregate the young from the elderly subjects. Compared with the classification performed earlier using the descriptive statistics, with the addition of indices like %REC, %DET, %LAM, r_{opt}^{min}, r_{opt}^{max}, and newly defined R_D, significant improvement in the quantification and classification of HRV is observed. Feature classification methods can be employed in future to optimize the choice of extracted features to successfully classify the HRV.

Compliance with ethical standards

The study abides by the ethical standards and was approved by the research advisory committee of the Inder Kumar Gujral Punjab Technical University, Punjab, India, and informed permission was obtained from all the subjects.

References

1. Guidelines (1996) Guidelines Heart rate variability. Eur Hear J 17: 354–381. https://doi.org/10.1161/01.CIR.93.5.1043

2. Acharya UR, Joseph KP, Kannathal N et al (2006) Heart rate variability: a review. Med Biol Eng Comput 44:1031–1051. https://doi.org/10.1007/s11517-006-0119-0
3. Sassi R, Cerutti S, Lombardi F, Malik M, Huikuri HV, Peng CK, Schmidt G, Yamamoto Y, Document Reviewers, Gorenek B, Lip GYH, Grassi G, Kudaiberdieva G, Fisher JP, Zabel M, Macfadyen R (2015) Advances in heart rate variability signal analysis: joint position statement by the e-Cardiology ESC Working Group and the European Heart Rhythm Association co-endorsed by the Asia Pacific Heart Rhythm Society. Europace 17:1341–1353. https://doi.org/10.1093/europace/euv015
4. Kaplan DT, Furman MI, Pincus SM, Ryan SM, Lipsitz LA, Goldberger AL (1991) Aging and the complexity of cardiovascular dynamics. Biophys J 59:945–949. https://doi.org/10.1016/S0006-3495(91)82309-8
5. Li X, Yu S, Chen H, Lu C, Zhang K, Li F (2015) Cardiovascular autonomic function analysis using approximate entropy from 24-h heart rate variability and its frequency components in patients with type 2 diabetes. J Diabetes Investig 6:227–235. https://doi.org/10.1111/jdi.12270
6. Singh A, Saini BS, Singh D (2016) A new baroreflex sensitivity index based on improved Hilbert-Huang transform for assessment of baroreflex in supine and standing postures. Biocybern Biomed Eng 36:355–365. https://doi.org/10.1016/j.bbe.2016.01.006
7. Shiogai Y, Stefanovska A, McClintock PVEE (2010) Nonlinear dynamics of cardiovascular ageing. Phys Rep 488:51–110. https://doi.org/10.1016/j.physrep.2009.12.003
8. Javorka M, Trunkvalterova Z, Tonhajzerova I, Javorkova J, Javorka K, Baumert M (2008) Short-term heart rate complexity is reduced in patients with type 1 diabetes mellitus. Clin Neurophysiol 119:1071–1081. https://doi.org/10.1016/j.clinph.2007.12.017
9. Castiglioni P, Parati G, Di Rienzo M et al (2011) Scale exponents of blood pressure and heart rate during autonomic blockade as assessed by detrended fluctuation analysis. J Physiol 589:355–369. https://doi.org/10.1113/jphysiol.2010.196428
10. Tulppo MP, Mäkikallio TH, Seppänen T et al (2001) Effects of pharmacological adrenergic and vagal modulation on fractal heart rate dynamics. Clin Physiol 21:515–523. https://doi.org/10.1046/j.1365-2281.2001.00344.x
11. Singh A, Saini BS, Singh D (2015) Multiscale joint symbolic transfer entropy for quantification of causal interactions between heart rate and blood pressure variability under postural stress. Fluct Noise Lett 14:1550031. https://doi.org/10.1142/S0219477515500315
12. Catai AM, Takahashi ACM, Perseguini NM, Milan J, Minatel V, Rehder-Santos P, Marchi A, Bari V, Porta A (2014) Effect of the postural challenge on the dependence of the cardiovascular control complexity on age. Entropy 16:6686–6704. https://doi.org/10.3390/e16126686
13. Orini M, Laguna P, Mainardi L, et al (2011) Characterization of the dynamic interactions between cardiovascular signals by cross time-frequency analysis: phase differences, time delay and phase locking. In: International Conference on Numerical Method in Engineering
14. Orini M, Laguna P, Mainardi LT, Bailón R (2012) Assessment of the dynamic interactions between heart rate and arterial pressure by the cross time-frequency analysis. Physiol Meas 33:315–331. https://doi.org/10.1088/0967-3334/33/3/315
15. Watanabe E, Kiyono K, Hayano J, Yamamoto Y, Inamasu J, Yamamoto M, Ichikawa T, Sobue Y, Harada M, Ozaki Y (2015) Multiscale entropy of the heart rate variability for the prediction of an ischemic stroke in patients with permanent atrial fibrillation. PLoS One 10:1–13. https://doi.org/10.1371/journal.pone.0137144
16. Akselrod S, Gordon D, Ubel F et al (1981) Power spectrum analysis of heart rate fluctuation: a quantitative probe of beat-to-beat cardiovascular control. Science (80-) 213:220–222. https://doi.org/10.1126/science.6166045
17. Orini M, Bailon R, Mainardi LT, Laguna P, Flandrin P (2012) Characterization of dynamic interactions between cardiovascular signals by time-frequency coherence. IEEE Trans Biomed Eng 59:663–673. https://doi.org/10.1109/TBME.2011.2171959
18. Brennan M, Palaniswami M, Kamen P (2001) Do existing measures of Poincareé plot geometry reflect nonlinear features of heart rate variability? IEEE Trans Biomed Eng 48:1342–1347. https://doi.org/10.1109/10.959330
19. Richman JS, Moorman JR, Yamauchi M et al (2011) Physiological time-series analysis using approximate entropy and sample entropy. Cardiovasc Res:2039–2049
20. Lake DE (2006) Renyi entropy measures of heart rate Gaussianity. IEEE Trans Biomed Eng 53:21–27. https://doi.org/10.1109/TBME.2005.859782
21. Voss A, Schulz S, Schroeder R, Baumert M, Caminal P (2009) Methods derived from nonlinear dynamics for analysing heart rate variability. Philos Trans R Soc A Math Phys Eng Sci 367:277–296. https://doi.org/10.1098/rsta.2008.0232
22. Rawal K, Saini BS, Saini I (2015) Adaptive correlation dimension method for analysing heart rate variability during the menstrual cycle. Australas Phys Eng Sci Med 38:509–523. https://doi.org/10.1007/s13246-015-0369-y
23. Arcentales A, Giraldo BF, Caminal P, et al (2011) Recurrence quantification analysis of heart rate variability and respiratory flow series in patients on weaning trials. 2011 Annu Int Conf IEEE Eng Med Biol Soc 2724–2727 . https://doi.org/10.1109/IEMBS.2011.6090747
24. Beckers F (2006) Aging and nonlinear heart rate control in a healthy population. Am J Physiol Heart Circ Physiol 290:H2560–H2570. https://doi.org/10.1152/ajpheart.00903.2005
25. Iyengar N, Peng CK, Morin R et al (1996) Age-related alterations in the fractal scaling of cardiac interbeat interval dynamics. Am J Phys 271:R1078–R1084
26. Kampouraki A, Manis G, Nikou C (2009) Heartbeat time series classification with support vector machines. IEEE Trans Inf Technol Biomed 13:512–518. https://doi.org/10.1109/TITB.2008.2003323
27. Manikandan MS, Soman KP (2012) A novel method for detecting R-peaks in electrocardiogram (ECG) signal. Biomed Signal Process Control 7:118–128. https://doi.org/10.1016/j.bspc.2011.03.004
28. Singh A, Saini BS, Singh D (2016) An alternative approach to approximate entropy threshold value (r) selection: application to heart rate variability and systolic blood pressure variability under postural challenge. Med Biol Eng Comput 54:723–732. https://doi.org/10.1007/s11517-015-1362-z
29. Webber CL, Zbilut JP (2005) Recurrence quantification analysis of nonlinear dynamical systems. In: Riley M, Van Orden G (eds.) Tutorials in Contemporary Nonlinear Methods for the Behavioral Sciences (pp. 26–94). USA: National Science Foundation
30. Webber CL, Marwan N (2015) Recurrence Quantification Analysis: Theory and Best Practices, 1st ed. Springer International Publishing
31. Orhan U, Hekim M, Ozer M (2011) EEG signals classification using the K-means clustering and a multilayer perceptron neural network model. Expert Syst Appl 38:13475–13481. https://doi.org/10.1016/j.eswa.2011.04.149
32. Subasi A (2005) Automatic recognition of alertness level from EEG by using neural network and wavelet coefficients. Expert Syst Appl 28:701–711. https://doi.org/10.1016/j.eswa.2004.12.027
33. Oğulata SN, Şahin C, Erol R (2009) Neural network-based computer-aided diagnosis in classification of primary generalized epilepsy by EEG signals. J Med Syst 33:107–112. https://doi.org/10.1007/s10916-008-9170-8
34. Hazarika N, Chen JZ, Tsoi AC, Sergejew A (1997) Classification of EEG signals using the wavelet transform. Proc 13th Int Conf Digit Signal Process 1:61–72 . https://doi.org/10.1016/S0165-1684(97)00038-8

35. Lee H, Shin S-Y, Seo M, Nam GB, Joo S (2016) Prediction of ventricular tachycardia one hour before occurrence using artificial neural networks. Sci Rep 6:32390. https://doi.org/10.1038/srep32390
36. Jan SU, Lee Y-D, Shin J, Koo I (2017) Sensor fault classification based on support vector machine and statistical time-domain features. IEEE Access 5:8682–8690. https://doi.org/10.1109/ACCESS.2017.2705644
37. Zhang L, Xiong G, Liu H, Zou H, Guo W (2010) Applying improved multi-scale entropy and support vector machines for bearing health condition identification. Proc Inst Mech Eng Part C J Mech Eng Sci 224:1315–1325. https://doi.org/10.1243/09544062JMES1784
38. Babaoglu İ, Findik O, Ülker E (2010) A comparison of feature selection models utilizing binary particle swarm optimization and genetic algorithm in determining coronary artery disease using support vector machine. Expert Syst Appl 37:3177–3183. https://doi.org/10.1016/j.eswa.2009.09.064
39. Porta A, Catai AM, Takahashi ACM, Magagnin V, Bassani T, Tobaldini E, van de Borne P, Montano N (2011) Causal relationships between heart period and systolic arterial pressure during graded head-up tilt. Am J Physiol Regul Integr Comp Physiol 300:R378–R386. https://doi.org/10.1152/ajpregu.00553.2010
40. Schinkel S, Dimigen O, Marwan N (2008) Selection of recurrence threshold for signal detection. Eur Phys J Spec Top 164:45–53. https://doi.org/10.1140/epjst/e2008-00833-5
41. Lu S, Chen X, Kanters JK et al (2008) Automatic selection of the threshold value r for approximate entropy. IEEE Trans Biomed Eng 55:1966–1972. https://doi.org/10.1109/TBME.2008.919870
42. Chon K, Scully C, Lu S (2009) Approximate entropy for all signals. IEEE Eng Med Biol Mag 28:18–23. https://doi.org/10.1109/MEMB.2009.934629
43. Ding H, Crozier S, Wilson S (2007) A new heart rate variability analysis method by means of quantifying the variation of nonlinear dynamic patterns. IEEE Trans Biomed Eng 54:1590–1597. https://doi.org/10.1109/TBME.2007.893495
44. García-González MA, Fernández-Chimeno M, Ramos-Castro J (2009) Errors in the estimation of approximate entropy and other recurrence-plot-derived indices due to the finite resolution of RR time series. IEEE Trans Biomed Eng 56:345–351. https://doi.org/10.1109/TBME.2008.2005951
45. Pincus SM (1991) Approximate entropy as a measure of system complexity. Proc Natl Acad Sci 88:2297–2301. https://doi.org/10.1073/pnas.88.6.2297
46. Daskalov I, Christov I (1997) Improvement of resolution in measurement of electrocardiogram RR intervals by interpolation. Med Eng Phys 19:375–379. https://doi.org/10.1016/S1350-4533(96)00067-7
47. Voss A, Heitmann A, Schroeder R, Peters A, Perz S (2012) Short-term heart rate variability—age dependence in healthy subjects. Physiol Meas 33:1289–1311. https://doi.org/10.1088/0967-3334/33/8/1289
48. Schipke JD, Pelzer M, Arnold G (1999) Effect of respiration rate on short-term heart rate variability. J Clin Basic Cardiol 2:92–95. https://doi.org/10.1161/01.CIR.93.5.1043
49. Voss A, Schroeder R, Fischer C, et al (2013) Influence of age and gender on complexity measures for short term heart rate variability analysis in healthy subjects. 35th Annu Int Conf IEEE 5574–5577 . https://doi.org/10.1109/EMBC.2013.6610813
50. Accardo A, D'Addio G, Maestri R, et al (2015) Fractal dimension and power-law behavior reproducibility and correlation in chronic heart failure patients. Eur Signal Process Conf 2015–March
51. Weippert M, Behrens M, Rieger A, Behrens K (2014) Sample entropy and traditional measures of heart rate dynamics reveal different modes of cardiovascular control during low intensity exercise. Entropy 16:5698–5711. https://doi.org/10.3390/e16115698

Vikramjit Singh is currently pursuing Ph.D. from I K G Punjab Technical University. His research areas are Biomedical Signal Processing, Non-linear Systems, and Digital Image Processing.

Dr. Amit Gupta is Assistant Professor in I K G Punjab Technical University, India, and has a Ph.D. in Electronics and Communication Engineering.

Dr. J.S. Sohal Director of Ludhiana College of Engineering and Technology, India, is a Ph.D. in Electronics from IIT, Roorkee, India. He is Ex. Prof & Head, Guru Nanak Dev University, India.

Dr. Amritpal Singh is Assistant Professor in I K G Punjab Technical University, India, and has a Ph.D. in Electronics. His research areas are Biomedical Signal Processing, Non-Linear Dynamics & Control.